Resonance ultrasonic actuation and local structural rejuvenation in metallic glasses

D. P. Wang,[1,2] Y. Yang,[1] X. R. Niu,[1] J. Lu,[1] G. N. Yang,[1,3] W. H. Wang,[2,*] and C. T. Liu[1,†]
[1]*Centre for Advanced Structural Materials, Department of Mechanical and Biomechanical Engineering, City University of Hong Kong, Hong Kong, China*
[2]*Institute of Physics, Chinese Academy of Sciences, Beijing, China*
[3]*School of Materials Science and Engineering, Tsinghua University, Beijing, China*
(Received 4 August 2016; published 6 June 2017)

Using the method of contact resonance ultrasonic actuation (CRUA), we observed evidence of local structural rejuvenation at the surface of metallic glasses (MGs), arising from the increase of the vibration amplitude of the atoms after the resonance actuation. By adjusting the CRUA parameters, the size, pattern, and extent of the rejuvenated zones could be tailored. Nanoindentation tests revealed suppressed nucleation of shear bands after CRUA, originating from the homogenization of the local structure induced by the ultrasonic vibration. Compared with the structural homogenization from annealing, this method will not sacrifice the concentration of the free volume for the local structural constraint. These results are useful to understand the evolution of the microstructure and local structural rejuvenation of MGs, as well as the design of MGs with improved plasticity from the nanoscale to the microscale.

DOI: 10.1103/PhysRevB.95.235407

I. INTRODUCTION

Metallic glasses (MGs) are structurally disordered solids with many unique properties and widespread potential applications [1–3]. Slow structural relaxation processes or physical aging are often observed to occur below the glass transition temperature for the state of thermal nonequilibrium [4,5]. Because of the gradual changes of the structure and properties of MGs associated with physical aging, this phenomenon has great interest. A strong connection has been demonstrated between physical aging and the mechanical behavior of MGs [6–8]. However, the annihilation of the free-volume or loose-packing regions during the aging process will lead to the glasses being even more brittle [7,8]. In the opposite direction of the aging process, structural rejuvenation is pretty crucial since it is also closely related to the mechanical properties of MGs, such as the improved compressive plasticity from thermal cycling [9–12]. These studies have promoted the understanding of the global structural rejuvenation of MGs. However, the local or the surface structural rejuvenation has not been investigated even though they are also important for the understanding and applications of MGs.

In this study, the method of contact resonance ultrasonic actuation (CRUA) was performed to tailor the microstructure with different rejuvenation behaviors at the surface of MGs. As an intrinsic structural parameter of MGs, the elastic modulus was selected as a metric to characterize the structural change since it has a widely approved correlation with the concentration of the loose-packing regions and properties of MGs: the microstructure of MGs can be considered as consisting of two parts: loose-packing regions embedded on dense-packing regions [13–22]; with the increase of the concentration of the loose-packing regions, the elastic modulus is expected to decrease accordingly (see Supplemental Material for the detailed relationship [23]).

*whw@iphy.ac.cn
†chainliu@cityu.edu.hk

II. EXPERIMENTS

Two kinds of MGs were selected with compositions of $Cu_{50}Zr_{50}$ and $Zr_{52.5}Cu_{17.9}Al_{10}Ni_{14.6}Ti_5$ (at.%). The ribbon samples with a cross section of 2.0 mm × 0.05 mm were prepared using a melt spinning method. The fully glassy structure of the ribbons was confirmed by x-ray diffraction (XRD; Bruker D8 ADVANCE; Cu $K\alpha$) and differential scanning calorimetry (DSC; Perkin-Elmer DSC 8000) as shown in Figs. S1 and S2 [23]. The details of CRUA can be seen in the Supplemental Material [23]. All atomic force microscope (AFM) images were obtained using a scanning rate of 1 Hz and in a 256 × 256 pixel data array. The nanoindentation experiments were carried out at a constant strain rate of $0.2\,s^{-1}$, using the Hysitron Nanoindentation System TI 950 and a spherical tip with a radius of 2.2 μm. The load-displacement curves were measured in square CRUA areas with a size of 20 μm. The width of the indentation test is about 1.2 μm, which is more than one order lower than the size of CRUA zones. Thirty data points were measured for the statistical analysis.

III. RESULTS AND DISCUSSION

A. Local structural rejuvenation

Figure 1(a) presents a schematic of the structural change using CRUA, where the elastic modulus can be calculated from the damped harmonic oscillator model corresponding to the loose and dense packing regions [15,24,25]. The height profile in Fig. 1(b) shows that the surface roughness of the samples is less than 1 nm, which is ideal for further research using AFM since the influence from the surface fluctuation can be negligible [17]. After CRUA, the topology of the sample is changed less than one atomic layer. However, the resonance frequency decreased by about 2 kHz for the same positions in Fig. 1(c), corresponding to the decrease of the elastic modulus [24]. More quantitative description of the elastic modulus is shown in Fig. S3 [23]. It can be seen that the elastic modulus decreased by 4 ± 1 GPa at the positions after CRUA,

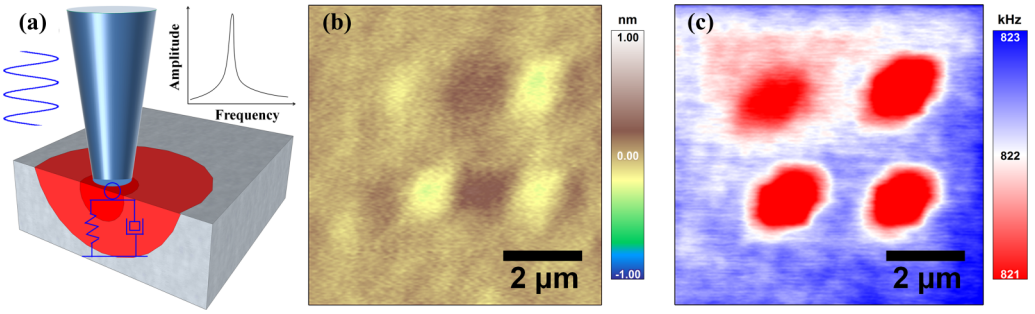

FIG. 1. (a) Schematic illustration of CRUA and the probe-sample contact system. The damped harmonic oscillator represents the viscoelastic nature of the probe-sample contact dynamics. (b) AFM topographic image of the metallic glassy ribbon after 5 CRUA; the surface roughness is less than 1 nm and the changed depth is less than one atomic layer. (c) Map of the contact resonance frequency of the sample after CRUA for four positions. All the images were scanned with 256 × 256 points, using a probe with a radius of 10 nm.

suggesting a higher global concentration of the loose-packing regions and local structural rejuvenation. In addition, this result can further confirm that the microstructure of MGs is heterogeneous in nature, and the degree of the heterogeneity is changeable. One important point to stress is that, in our AFM measurement with 256 × 256 points, since the radius of the probe (∼10 nm) is larger than the characteristic length of the heterogeneity of MGs (<10 nm) [16], several loose and dense packing regions will be detected for each measurement point at the same time. Therefore, the respective elastic information of the two individual regions is unavailable, and only a complex effect of the two regions could be obtained. However, based on the structural model of MGs [13–20,22], from the complex modulus of the detected regions at a scale of tens of nanometers, the relative fraction of the loose-packing regions can be deduced, especially for the trend of the change of their concentration [23].

Many aspects of the structural rejuvenation could be tailored from CRUA parameters, such as the number of the treatments, and the size and distribution of the rejuvenated zones. By changing the number of the treatments, the extent of the structural rejuvenation could be altered. In Fig. 2(a),

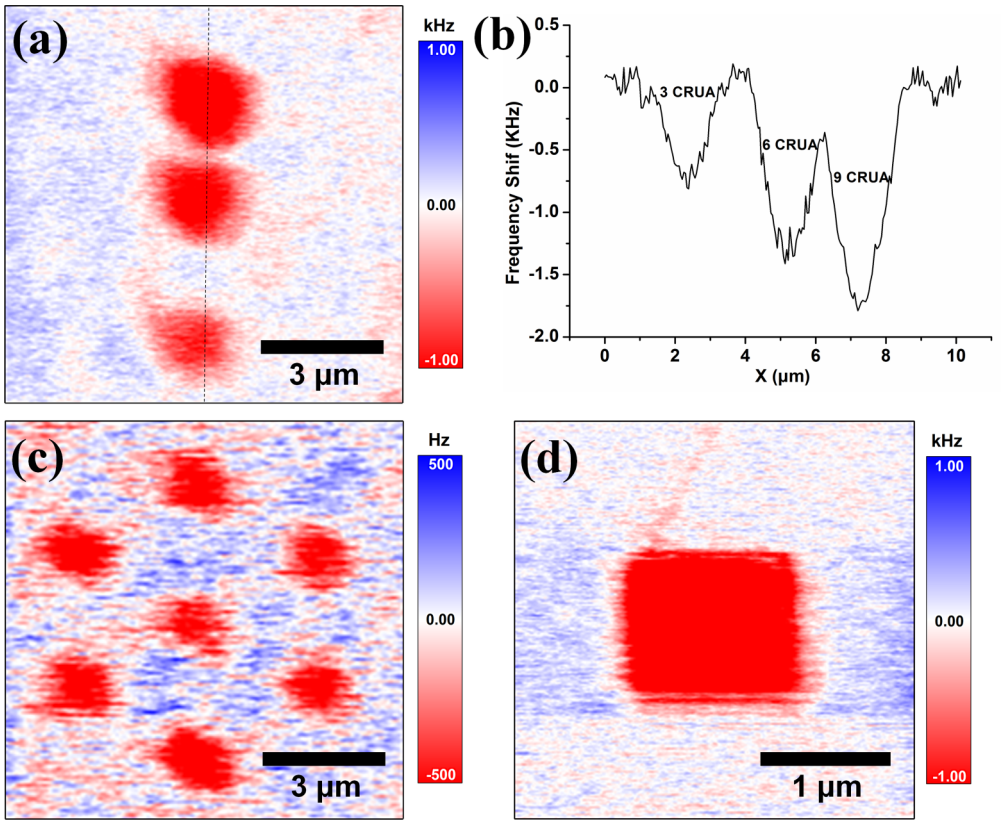

FIG. 2. (a) The controlling of the extent of the rejuvenated zones by changing the CRUA number: from top to bottom, the number of the treatments decreased from 9, 6, to 3. (b) The contact resonance frequency shift of the sample after CRUA with different times, corresponding to the dotted line in (a). The design of the distribution (c) and size (d) of the rejuvenated zones by changing the CRUA parameters.

from the top to bottom, the red sites were scanned separately for different times, i.e., 9, 6, and 3. It can be seen that, with an increasing number of treatments, the resonance frequency shifted to lower values. This result indicates that with the increasing of times, more loose-packing regions can be activated. What is more, by controlling the position and size of the treatment, the pattern and size of the rejuvenated zones can also be controlled, as shown in Figs. 2(c) and 2(d) and Fig. S4 [23].

In addition, as indicated in Fig. S5, this method is also suitable for other kinds of MGs, such as $Zr_{52.5}Cu_{17.9}Al_{10}Ni_{14.6}Ti_5$ ribbons, since the MGs have the same metastable microstructure in the nonequilibrium state and the energy state could be changed by ultrasonic actuation [23]. One issue should be pointed out is that, depending on the composition, fabrication route, and other parameters, and although there is an absence of long-range order, the local environment around each atom and configurations of the local structure can vary, as well as the degree of the heterogeneity or the short-to-medium range order of the amorphous structure. Therefore, the local microstructure of MGs can be various from one system to another. For example, the correlation length of the heterogeneity of a $Zr_{55}Cu_{30}Ni_5Al_{10}$ MG film was measured to be ~2.5 nm [16], but the local modulus distribution and structural heterogeneity can be obtained at a scale of 10 nm for a $Pd_{77.5}Cu_{6.0}Si_{16.5}$ MG ribbon [17]. Therefore, the absolute response to the actuation could also be various, depending on the initial structure of a special system.

B. Mechanism of the local structural rejuvenation

We explain the local structural rejuvenation from the increase of the vibration amplitude of the atoms after the resonance actuation. For condensed matter in the liquid state, the vibration amplitude of atoms is large and the packing density is low. With the decrease of the temperature, the vibration amplitude also decreases [5,11,26,27]. In our experiment, the sample is vibrating at a high frequency, as high as MHz, and it contacts with the probe in the model of resonance vibration [24,28]. As we know, in the state of resonance, the vibration amplitude of atoms will increase suddenly to a large value. For MGs under the resonance actuation and the force from the probe, the atoms with large vibration amplitude will reach to higher energy states in the energy landscape [27]. Compared with the untreated sites, the packing density of sites after CRUA is decreased. After the resonance, the activated heterogeneity will be confined by the structure around it and more loose-packing regions will be obtained, which leads to the decrease of the elastic modulus and increase of the effective amount of the loose-packing regions, as presented in the box of Fig. 3(c) [12]. Another possible reason for the structural rejuvenation is the energy input into the sample from the high-frequency vibration under the force of the probe [29].

C. Mechanical properties after the local structural rejuvenation

Structural heterogeneity plays a key role in the mechanical behavior of MGs [12,30–33]. To get more information about the influence of CRUA on the mechanical properties of MGs,

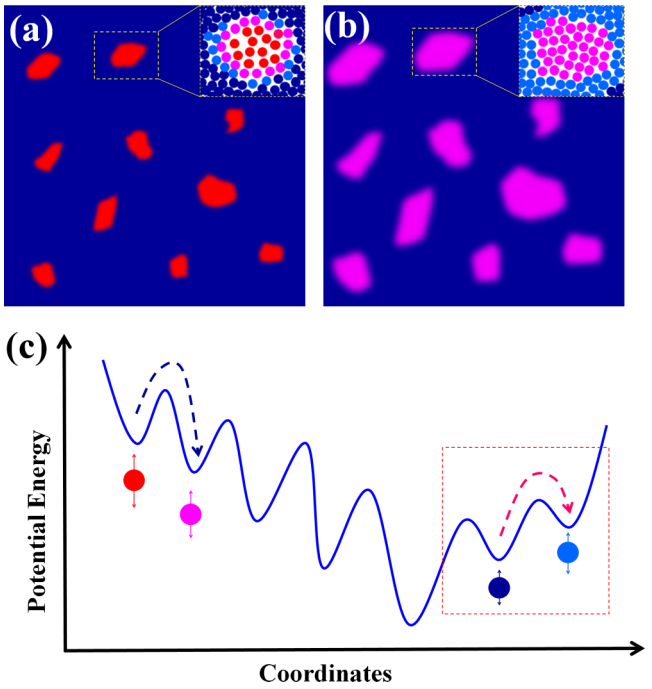

FIG. 3. (a) Schematic illustration of the microstructure and energy states of the atoms for the as-cast sample. The positions in the energy landscape decrease from red, pink, light blue, to blue spheres. The high-mobility atoms (red spheres) embedded in the elastic shell (blue spheres). (b) The microstructure and energy states of the atoms after CRUA. More loose-packing regions are activated near the relaxed loose-packing cores and the microstructure becomes more homogeneous. (c) The change of the positions in the energy landscape of the atoms in the MG during CRUA: the loose-packing cores relaxed to a lower energy state, which leads to an increasing of the critical load of the shear bands initiation; the atoms of the peripheral dense-packing matrix jumped to a higher energy state, which leads to a decrease of the elastic modulus.

representative load-displacement curves and the statistical data are presented in Fig. 4. It can be seen that the critical load at the first pop-in for the sites after CRUA is about 200 μN higher than that of the as-cast one. This means that a higher load is required to trigger the first shear band event. As mentioned in previous studies [34–37], upon mechanical loading, local plastic events, or shear transformations, will occur at the loose-packing regions. When the load reaches a critical value, a liquid layer with an initiation viscosity of 10^8 Pa s could form by coalescence of the loose-packing regions, regarded as the nucleation of shear bands in MGs. To compensate the volume change during CRUA, the original loose-packing cores with the high-energy state will relax to states with lower energies. This evolution could be considered as a coupled process of rejuvenation in the dense-packing matrix and relaxation in the loose-packing cores. As the nucleation sites of shear bands or the weakest portions in MGs, the viscosity of the loose-packing cores will be higher after CRUA. Therefore, a higher critical stress for shear band nucleation from these points could be expected since the original loose-packing cores were relaxed after CRUA [38–42]. The suppression of the heterogeneous nucleation of shear bands from the homogenization effect

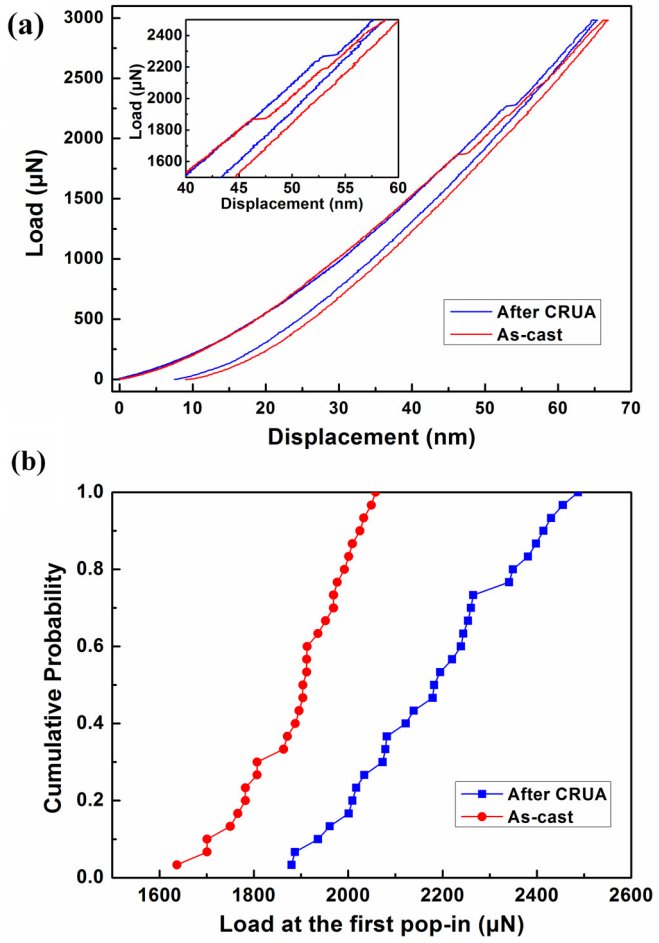

FIG. 4. (a) Representative load-displacement curves from nanoindentation measurements for the samples after 5 CRUA and the as-cast one. (b) Statistical data of the critical load at the first pop-in from nanoindentation for the samples showing an increase of the strain capacity after CRUA.

has also been reported in annealing experiments, where only relaxation happened [7,39].

D. Potential and extending applications of CRUA

Structural rejuvenation has been pursued for a long time for its correlation with the properties of MGs [12,31,43,44]. Here, the method of CRUA has been used to achieve the local structural rejuvenation from the nanoscale to the microscale. In addition, the size, extent, and pattern of the rejuvenated zones can be tuned at the surface of the samples, which hints that the microstructure of MGs could be tailored as required. Proceeding from the elastic perspective, our study provides a simple and efficient method to tailor the microstructure and properties at the local surface of MGs, such as the strength, hardness, and other mechanical properties, since they are closely correlated with the elastic modulus [45]. What is more, this is a promising method to improve the plasticity of MGs at the microscale for the local structural rejuvenation and the designed parameter of the rejuvenated zones since the glasses can be considered as consisting of different glassy phases with various degree of heterogeneity [46]. Beyond the applications in the field of MGs, CRUA has also been used to tailor the surface properties of the polycrystalline thin film using photothermal excitation after the developed voltage spectroscopy [47]. Extending from these studies, more CRUA methods can be envisaged for probing the nanomechanical behavior of materials under other types of applied impulses. In addition, the theory and principle can also be potentially extended to the bulk condition. For example, the viscosity of the bulk MGs can be decreased significantly using the ultrasonic beating method [29].

E. Possible correlation with the β relaxation

The β relaxation has been linked to the evolution of loose-packing regions, which is correlated with the mechanical and dynamics behavior of MGs [30,48]. With the increase of temperature, the β relaxation can be activated since the dense-packing regions around loose-packing cores are gradually transformed into a loose-packing state, resulting in an increase of the fraction of the loose-packing regions [30]. From the relaxation spectra of glass-forming materials, the β relaxation can also be activated by high-frequency vibration [49]. In our work, the frequency of CRUA is close to the intrinsic vibration frequency corresponding to the β relaxation of MGs ($10^5 - 10^6$ Hz) [49]. The structural evolution from CRUA is similar with the thermal-activated β relaxation, but there is only a coordination of the volume between the loose-packing and dense-packing regions. In addition, this evolution is irreversible at room temperature for the constraint of the local structure from the peripheral part without CRUA and the ultrafast CRUA process [50]. Therefore, this clue may offer a way to understand the β relaxation of MGs from the perspective of the frequency.

IV. CONCLUSION

The method of CRUA was used to gain the local structural rejuvenation of MGs. The elastic modulus and nanoindentation tests indicated a simultaneous rejuvenation in the dense-packing regions and relaxation in the loose-packing regions during the CRUA process. The rejuvenation in the dense-packing regions leads to the decrease of the elastic modulus and the relaxed loose-packing cores can suppress the nucleation of the first shear band. In addition, the size, extent, and pattern of the rejuvenated zones could be tuned as required. Therefore, CRUA will be a simple and attractive method to tailor the local microstructure and properties of MGs since they are closely related to the elastic modulus.

ACKNOWLEDGMENTS

Technical support from Asylum Research and helpful discussions with Dr. Z. G. Zhu and Dr. B. A. Sun are greatly appreciated. This work was supported by the General Research Fund (GRF) of the Hong Kong Government (Grant No. CityU 102013), the NSF of China (Grants No. 51571209 and No. 51461165101), and the MOST 973 Program (No. 2015CB856800).

[1] A. L. Greer, Science **267**, 1947 (1995).
[2] W. H. Wang, C. Dong, and C. H. Shek, Mater. Sci. Eng. R **44**, 45 (2004).
[3] M. F. Ashby and A. L. Greer, Scr. Mater. **54**, 321 (2006).
[4] A. Van den Beukel and S. Radelaar, Acta Metall. **31**, 419 (1983).
[5] H. S. Chen and E. Coleman, Appl. Phys. Lett. **28**, 245 (1976).
[6] J. J. Lewandowski, W. H. Wang, and A. L. Greer, Philos. Mag. Lett. **85**, 77 (2005).
[7] W. D. Li, Y. F. Gao, and H. B. Bei, Sci. Rep. **5**, 14786 (2015).
[8] G. Kumar, D. Rector, R. D. Conner, and J. Schroers, Acta Mater. **57**, 3572 (2009).
[9] F. Q. Meng, K. Tsuchiya, I. Seiichiro, and Y. Yokoyama, Appl. Phys. Lett. **101**, 121914 (2012).
[10] Y. Tong, T. Iwashita, W. Dmowski, H. Bei, Y. Yokoyama, and T. Egami, Acta Mater. **86**, 240 (2015).
[11] M. Utz, P. G. Debenedetti, and F. H. Stillinger, Phys. Rev. Lett. **84**, 1471 (2000).
[12] S. V. Ketov, Y. H. Sun, S. Nachum, Z. Lu, A. Checchi, A. R. Beraldin, H. Y. Bai, W. H. Wang, D. V. Louzguine-Luzgin, M. A. Carpenter, and A. L. Greer, Nature (London) **524**, 200 (2015).
[13] T. Ichitsubo, S. Hosokawa, K. Matsuda, E. Matsubara, N. Nishiyama, S. Tsutsui, and A. Q. R. Baron, Phys. Rev. B **76**, 140201 (2007).
[14] W. Dmowski, T. Iwashita, C. P. Chuang, J. Almer, and T. Egami, Phys. Rev. Lett. **105**, 205502 (2010).
[15] J. C. Ye, J. Lu, C. T. Liu, Q. Wang, and Y. Yang, Nat. Mater. **9**, 619 (2010).
[16] Y. H. Liu, D. Wang, K. Nakajima, W. Zhang, A. Hirata, T. Nishi, A. Inoue, and M. W. Chen, Phys. Rev. Lett. **106**, 125504 (2011).
[17] H. Wagner, D. Bedorf, S. Küchemann, M. Schwabe, B. Zhang, W. Arnold, and K. Samwer, Nat. Mater. **10**, 439 (2011).
[18] B. A. Sun, Y. C. Hu, D. P. Wang, Z. G. Zhu, P. Wen, W. H. Wang, C. T. Liu, and Y. Yang, Acta Mater. **121**, 266 (2016).
[19] D. Srolovitz, K. Maeda, V. Vitek, and T. Egami, Philos. Mag. A **44**, 847 (1981).
[20] Z. Lu, W. Jiao, W. H. Wang, and H. Y. Bai, Phys. Rev. Lett. **113**, 045501 (2014).
[21] T. Ichitsubo, W. Itaka, E. Matsubara, H. Kato, S. Biwa, S. Hosokawa, K. Matsuda, J. Saida, O. Haruyama, Y. Yokoyama, H. Uchiyama, and A. Q. R. Baron, Phys. Rev. B **81**, 172201 (2010).
[22] J. Ding, S. Patinet, M. L. Falk, Y. Q. Cheng, and E. Ma, Proc. Natl. Acad. Sci. USA **111**, 14052 (2014).
[23] See Supplemental Material at http://link.aps.org/supplemental/10.1103/PhysRevB.95.235407 for experimental details and structural models of metallic glasses.
[24] U. Rabe, S. Amelio, E. Kester, V. Scherer, S. Hirsekorn, and W. Arnold, Ultrasonics **38**, 430 (2000).
[25] L. S. Huo, J. F. Zeng, W. H. Wang, C. T. Liu, and Y. Yang, Acta Mater. **61**, 4329 (2013).
[26] A. V. Granato, D. M. Joncich, and V. A. Khonik, Appl. Phys. Lett. **97**, 171911 (2010).
[27] P. G. Debenedetti and F. H. Stillinger, Nature (London) **410**, 259 (2001).
[28] G. Stan and W. Price, Rev. Sci. Instrum. **77**, 103707 (2006).
[29] J. Ma, X. Liang, X. Y. Wu, Z. Y. Liu, and F. Gong, Sci. Rep. **5**, 17844 (2015).
[30] Z. Wang, B. A. Sun, H. Y. Bai, and W. H. Wang, Nat. Commun. **5**, 5823 (2014).
[31] W. Dmowski, Y. Yokoyama, A. Chuang, Y. Ren, M. Umemoto, K. Tsuchiya, A. Inoue, and T. Egami, Acta Mater. **58**, 429 (2010).
[32] E. S. Park, J. S. Kyeong, and D. H. Kim, Scr. Mater. **57**, 49 (2007).
[33] Y. Q. Cheng and E. Ma, Phys. Rev. B **80**, 064104 (2009).
[34] B. A. Sun, Z. Y. Liu, Y. Yang, and C. T. Liu, Appl. Phys. Lett. **105**, 091904 (2014).
[35] Z. Y. Liu, Y. Yang, and C. T. Liu, Acta Mater. **61**, 5928 (2013).
[36] J. O. Krisponeit, S. Pitikaris, K. E. Avila, S. Küchemann, A. Krüger, and K. Samwer, Nat. Commun. **5**, 3616 (2014).
[37] X. L. Wang, F. Jiang, H. Hahn, J. Li, H. Gleiter, J. Sun, and J. X. Fang, Scr. Mater. **116**, 95 (2016).
[38] A. S. Argon and L. T. Shi, Acta Metall. **31**, 499 (1983).
[39] A. J. Cao, Y. Q. Cheng, and E. Ma, Acta Mater. **57**, 5146 (2009).
[40] B. A. Sun, Y. Yang, W. H. Wang, and C. T. Liu, Sci. Rep. **6**, 21388 (2016).
[41] C. A. Schuh and T. G. Nieh, Acta Mater. **51**, 87 (2003).
[42] Y. Q. Cheng and E. Ma, Acta Mater. **59**, 1800 (2011).
[43] M. Stolpe, J. J. Kruzic, and R. Busch, Acta Mater. **64**, 231 (2014).
[44] S. G. Mayr, Phys. Rev. B **71**, 144109 (2005).
[45] W. H. Wang, Prog. Mater. Sci. **57**, 487 (2012).
[46] B. Sarac and J. Schroers, Nat. Commun. **4**, 2158 (2013).
[47] Q. Li, S. Jesse, A. Tselev, L. Collins, P. Yu, I. Kravchenko, S. V. Kalinin, and N. Balke, ACS Nano **9**, 1848 (2015).
[48] H. B. Yu, W. H. Wang, H. Y. Bai, Y. Wu, and M. W. Chen, Phys. Rev. B **81**, 220201 (2010).
[49] P. Lunkenheimer, U. Schneider, R. Brand, and A. Loid, Contemp. Phys. **41**, 15 (2000).
[50] H. B. Yu, W. H. Wang, and K. Samwer, Mater. Today **16**, 183 (2013).